A two-step optimisation approach for the design of composite stiffened panels Part II: optimal design of the laminate

Marco Montemurro, Angela Vincenti, Paolo Vannucci

A two-step optimisation approach for the design of composite stiffened panels
Part II: optimal design of the laminate

M. Montemurro

Institut d'Alembert UMR7190 CNRS -Université Pierre et Marie Curie Paris 6,
Case 162, 4, Place Jussieu, 75252 Paris Cedex 05, France and
Centre de Recherche Public Henri Tudor, av. 29, J.F. Kennedy, L-1855 Luxembourg-Kirchberg, Luxembourg.

A. Vincenti

Institut d'Alembert UMR7190 CNRS - Université Pierre et Marie Curie Paris 6,
Case 162, 4, Place Jussieu, 75252 Paris Cedex 05, France.

P. Vannucci*

Université de Versailles et St Quentin, 45 Avenue des Etats-Unis, 78035 Versailles, France.

Author for Correspondence:
Paolo Vannucci, Professor,
Université de Versailles et Saint Quentin-en-Yvelines,
45, Avenue des Etats-Unis,
78035 Versailles, France
tel: +33 1 39 25 30 20,
fax: +33 1 39 25 30 15,
e.mail: paolo.vannucci@uvsq.fr

*Corresponding author.

Abstract

This paper deals with the definition of an optimisation procedure for the design of the wing-box composite stiffened panels subject to compression loads. In particular, the objective is to obtain a minimum-weight structure ensuring, at the same time, that the first buckling load should be greater then or equal to a threshold value. The optimisation strategy is subdivided into two phases: in the first one, we perform the global optimisation of the whole structure in terms of geometrical and material design variables, while in the second one the design of the laminate (for both skin and stiffeners laminates) is performed in terms of the stacking sequence. Moreover, no simplifying hypotheses are made on the panel geometry and on the behaviour of the laminates, i.e. types of stacking sequences, which compose the structure and the usual mechanical requirements, such as uncoupling and bending orthotropy, are exactly fulfilled. The results concerning the first optimisation phase (structural optimisation) were discussed in a previous paper. In this work, we show the results of the second optimisation step, i.e. the results of the optimal design of laminates, having some peculiar elastic properties. The problem is stated as the unconstrained minimisation of a positive semi-definite function, whose absolute minimum is known a-priori and it is equal to 0. We show the numerical results for three representative cases: the first one concerns the wing-box section with identical stiffeners, the second one is about the wing-box section with non-identical stiffeners, while the last one is the wing box with non-identical stiffeners with a symmetric distribution of the geometrical and polar parameters.

1 Introduction

This is the second part of a study where an optimisation procedure for the design of the wing-box composite stiffened panel subject to compression loads has been developed. This strategy was originally conceived for the optimal design of the anisotropy of composite laminated structures with variable stiffness, see [1, 2, 3], and also for multi-physics problems of laminates [4]. We recall that the goal is to design a minimum-weight wing-box structure considering a constraint on the first buckling load. The adopted strategy is subdivided into two phases: the first one concerns the optimisation of the whole structure in terms of geometrical and material design variables and it has been presented in the first part of this work. The second part concerns the design of the laminate, both for the skin and the stiffeners laminates, in terms of stacking sequences. This procedure is very general: during the whole process, no simplifying hypotheses are made on the panel geometry and on its mechanical behaviour.

It is worth noting that this is an innovative point of view and way of acting. In fact, usually the design of laminated structures is so difficult that designers use simplifying assumptions which automatically ensure some basic properties. The classical example is the use of balanced symmetric stacks. Symmetry is used to automatically obtain bending-extension uncoupling but, as it is suddenly recognised, it can seriously compromise the design of a lightweight structure. Balanced stacks ensure extension orthotropy but this assumption constitutes a serious limitation on the search for minimum weight structure. In addition, in the most part of works on buckling of laminates, it is considered to ensure, at least approximately, also bending orthotropy, very important for laminates buckling, but this is mechanically false, see [5]. All these rules can be avoided using a global optimisation strategy, leading on one side to the true global optimum, and on the other side able to satisfy all the requirements on the elastic behaviour of the laminate, like uncoupling, bending orthotropy and so on, see [6].

The results of the first optimisation phase, i.e. the structural optimisation of the whole wing-box section, were discussed in the first part of this work. This second part is focused on the stacking sequence design of the optimal laminates found in the first part. Also this problem is formulated as an optimisation problem, in particular as the search for the minima of a positive semi-definite quadratic form.

Several authors have considered different laminate design problems (rather complete but not exhaustive reviews on the state of the art can be found in [7, 8, 9]): see for instance the contribution of Werren and Norris [10] on isotropy, the works of Fukunaga [11], Paradies [12], Vannucci and Verchery [13] still on isotropy, those of Caprino and Crivelli-Visconti [14] and of Grédiac [15] on the orthotropy and, finally, those of Vannucci and Verchery [16, 17] on uncoupling and quasi-homogeneity. In particular, Vannucci [6] considered the problem of designing the elastic symmetries of the laminate. In that work a general approach based on polar tensor invariants was proposed: no simplifying hypotheses were made, and thus general solution could be found for a given problem. This approach was applied and extended in [5] for the constrained optimisation of laminated plates and in [1] for the optimal design of laminates with given elastic moduli.

The objective of this second part is to find the optimal stacking sequences, for the laminates of both the skin and the stiffeners, which give the values of the polar parameters obtained in the structural optimisation step. In this way, we are able to find a solution which automatically ensures the mechanical and geometrical properties of the whole structure, such as the behaviour of the laminates in terms of in-plane, coupling and

out-of-plane stiffness tensors, besides the global mechanical response of the whole wing-box section in terms of buckling load.

When dealing with the problem of designing the elastic symmetries of laminates, a basic question concerns the choice of the elastic tensor representation. Indeed, the Cartesian representation is not well suited to such a purpose, as symmetries appear clearly only for some particular choices of the reference frame. For this reason, the polar method seems to be a good choice to represent the classical stiffness tensors which describe the behaviour of the laminate: through this method an elastic tensor is known by five invariants and a parameter fixing the reference frame. Moreover, each invariant is related to a particular symmetry of the tensor. Under a mathematical point of view, the formulation of the design of laminate elastic symmetries, originally proposed by Vannucci [6], corresponds to the search for the absolute minimum of an unconstrained positive semi-definite function in the space of polar parameters, whose value is known *a-priori* and it is equal to 0. In addition the laminates for the skin and the stiffeners must be designed in order to match some given values of polar moduli corresponding to a specific elastic behaviour, which is optimal according to the results of the structural optimisation phase. The formulation of the optimal design of the laminate is modified in order to take into account all the requirements, simultaneously and without loss of generality, see [1].

In this work, no simplifying hypotheses are formulated on the types of stacking sequences used for skin and stiffeners laminates: no standard sequences, such as symmetric balanced, angle-ply or cross-ply sequences are employed. In this manner, we have no restriction on the ply's orientation and we perform a real global search of solutions: renouncing the use of standard stacking sequences leads to find some wing-box configurations which show a reduction of the weight of the whole structure up to 50%, when compared with a classical solution realised by aluminium alloy. Moreover, these configurations show good mechanical performances, in terms of pre-buckling stiffness and buckling loads. Concerning the optimisation tool, the genetic algorithm (GA) BIANCA [5, 18] was employed also in this second phase of the optimisation procedure, in order to find the best stacking sequences for our problem.

The paper is organised as follows: firstly, the mathematical background that we need in order to formulate the laminate design as an optimisation problem is presented in Sec. 2, while in Sec. 3 the formulation of the optimisation problem is described in details. The numerical results are discussed in Sec. 4 and, finally, in Sec. 5 we show a verification, via finite element (FE) analyses, of the optimal stacking sequences found at the end of the whole optimisation process.

2 General equations

The theoretical frame considered here is the Classical Laminated Plate Theory (CLPT) where the elastic behaviour of the laminate is described by three tensors: the in-plane, coupling and out-of-plane stiffness tensors, i.e. $\mathbf{A}$, $\mathbf{B}$ and $\mathbf{D}$ respectively.

Through the polar method we can give a representation of any planar tensor by means of its invariants. These invariants are called polar parameters and they have also a physical meaning, i.e. they are directly linked to the different symmetries of the tensor, see [19, 20].

Let us consider the reduced stiffness tensor of the lamina, $\mathbf{Q}$. In the framework of the polar representation, it is possible to express the Cartesian components of $\mathbf{Q}$ as:

$$
\begin{aligned}
Q_{11} &= T_0 + 2T_1 + R_0\cos 4\Phi_0 + 4R_1\cos 2\Phi_1 \,, \\
Q_{12} &= -T_0 + 2T_1 - R_0\cos 4\Phi_0 \,, \\
Q_{16} &= R_0\sin 4\Phi_0 + 2R_1\sin 2\Phi_1 \,, \\
Q_{22} &= T_0 + 2T_1 + R_0\cos 4\Phi_0 - 4R_1\cos 2\Phi_1 \,, \\
Q_{26} &= -R_0\sin 4\Phi_0 + 2R_1\sin 2\Phi_1 \,, \\
Q_{66} &= T_0 - R_0\cos 4\Phi_0 \,.
\end{aligned}
\tag{1}
$$

In eqs. (1) the Cartesian components of the ply's reduced stiffness tensor $\mathbf{Q}$ are expressed using Voigt's notation. T_0, T_1, R_0, R_1, $\Phi_0 - \Phi_1$ are the polar tensor invariants. T_0 and T_1 are the moduli related to the isotropic part of the tensor, R_0 and R_1 are the moduli related to anisotropic one, while Φ_0 and Φ_1 are the polar angles. For more details on the properties of polar parameters see [20].

In the framework of the CLPT, the in-plane, out-of-plane and coupling stiffness tensors of the laminate can be expressed in terms of polar parameters:

$$
\begin{aligned}
T_0^A, T_0^B, T_0^D &= \frac{1}{m}\sum_{k=1}^{n} T_{0k}\left(z_k^m - z_{k-1}^m\right), \\
T_1^A, T_1^B, T_1^D &= \frac{1}{m}\sum_{k=1}^{n} T_{1k}\left(z_k^m - z_{k-1}^m\right), \\
R_0^A \mathrm{e}^{4\mathrm{i}\Phi_0^A}, R_0^B \mathrm{e}^{4\mathrm{i}\Phi_0^B}, R_0^D \mathrm{e}^{4\mathrm{i}\Phi_0^D} &= \frac{1}{m}\sum_{k=1}^{n} R_{0k}\mathrm{e}^{4\mathrm{i}(\Phi_{0k}+\delta_k)}\left(z_k^m - z_{k-1}^m\right), \\
R_1^A \mathrm{e}^{2\mathrm{i}\Phi_1^A}, R_1^B \mathrm{e}^{2\mathrm{i}\Phi_1^B}, R_1^D \mathrm{e}^{2\mathrm{i}\Phi_1^D} &= \frac{1}{m}\sum_{k=1}^{n} R_{1k}\mathrm{e}^{2\mathrm{i}(\Phi_{1k}+\delta_k)}\left(z_k^m - z_{k-1}^m\right),
\end{aligned}
\tag{2}
$$

where T_0^A, T_1^A, R_0^A, R_1^A, Φ_0^A and Φ_1^A are the polar components of tensor $\mathbf{A}$, T_0^B, T_1^B, R_0^B, R_1^B, Φ_0^B and Φ_1^B are the polar components of tensor $\mathbf{B}$, while T_0^D, T_1^D, R_0^D, R_1^D, Φ_0^D and Φ_1^D are the polar components of tensor $\mathbf{D}$. In eqs. (2), m=1,2,3 for the extensional, coupling and bending stiffness tensor, respectively. T_{0k}, T_{1k}, R_{0k}, R_{1k}, Φ_{0k} and Φ_{1k} are the polar parameters of the reduced stiffness tensor of the k^{th} lamina; δ_k is the k^{th} ply's orientation measured with respect to the global frame of the laminate, n is the number of plies, while z_k and z_{k-1} are the z coordinates of the top and bottom k^{th} layer's surfaces. From eqs. (2), it can also be noticed that the symmetries of the laminate in terms of extension, coupling or bending behaviour depend on the stacking sequence, i.e. on layer's properties, orientation and thickness as well as the number of plies. Finally, we remark that expressions (1) are valid for any fourth-order elasticity-like tensor, so it is possible to apply this relation also to the $\mathbf{A}$, $\mathbf{B}$ and $\mathbf{D}$ stiffness tensors of the laminate.

3 Formulation of the optimisation problem for the laminate

When concerned with laminate's design, a designer has to satisfy, at the same time, several conditions including not only common objectives, like for instance buckling load or strength, but also general properties of the elastic response of the laminate, such as uncoupling, extension orthotropy, bending orthotropy and so on. As a matter of fact, it is not easy to take into account all these aspects, and, as already said, normally designers use some shortcuts to get automatically some properties like uncoupling or extension orthotropy. Vannucci and Vincenti have shown in previous studies (see [6, 5]) that it is possible, in the framework of the polar method, to formulate all the problems of optimal design of laminates including the requirements on elastic symmetries; therefore, a general approach to the design of laminates is actually possible.

In this paper we use uncoupled, homogeneous, fully-orthotropic laminates for both the skin and the stiffeners of the wing-box section. Introducing the homogenised stiffness tensors defined as:

$$\begin{aligned} \mathbf{A}^* &= \frac{1}{h_{lam}}\mathbf{A}, \\ \mathbf{B}^* &= \frac{2}{h_{lam}^2}\mathbf{B}, \\ \mathbf{D}^* &= \frac{12}{h_{lam}^3}\mathbf{D}, \\ \mathbf{C} &= \mathbf{A}^* - \mathbf{D}^*, \end{aligned} \tag{3}$$

the previous conditions can be expressed as:

$$\begin{aligned} \mathbf{B}^* &= \mathbf{O} \qquad \textit{uncoupling condition}, \\ \mathbf{C} &= \mathbf{O} \qquad \textit{homogeneity condition}, \\ \Phi_0^{A^*} - \Phi_1^{A^*} &= K^{A^*}\frac{\pi}{4} \qquad \textit{orthotropy condition}. \end{aligned} \tag{4}$$

If the two first conditions of eqs.(4) are satisfied, the laminate is said *quasi-homogeneous*, see [17]. In eqs. (3) h_{lam} is the global thickness of the laminate, while $\mathbf{C}$ is the homogeneity tensor which measures the difference between the in- and out-of-plane stiffness. In eqs. (4) $\Phi_0^{A^*}$ and $\Phi_1^{A^*}$ are the polar angles of tensor $\mathbf{A}^*$ and K^{A^*} can assume only the values 0 or 1, depending on the shape of orthotropy, [20]. It can be noticed that, if the laminate is homogeneous, and if tensor $\mathbf{A}^*$ is orthotropic then, due to the homogeneity condition, the tensor $\mathbf{D}^*$ is also orthotropic.

As previously said we can express the conditions of eqs. (4) in a synthetic way by stating the problem of the laminate design as an unconstrained minimisation problem of a positive semi-definite function, whose absolute minimum is known a-priori and it is equal to 0, see [6]. Since the aim of this second optimisation step is to find a stacking sequence (for every laminate composing the skin and the stiffeners) which satisfies the conditions of eqs. (4) together with the assigned value of polar parameters $R_0^{A^*}$, $R_1^{A^*}$, $\Phi_1^{A^*}$ and K^{A^*} found in the structural optimisation phase, we have to consider the presence of those terms in the unconstrained objective function.

We remind that the inputs of this second step of the optimisation process, i.e. the laminate design, are the thickness of the skin and stiffeners laminates besides the corresponding values of polar quantities $\widehat{R}_{0K}^{A^*}$ and $\widehat{R}_1^{A^*}$ issued from the first optimisation step. We recall here the relation among the polar parameters $\widehat{R}_0^{A^*}$ and $\widehat{K}^{A^*}$ and the polar quantity $\widehat{R}_{0K}^{A^*}$:

$$\widehat{R}_0^{A^*} = |\widehat{R}_{0K}^{A^*}| \ , \ \widehat{K}^{A^*} = \begin{cases} 0 & \text{if} \quad \widehat{R}_{0K}^{A^*} > 0 \\ 1 & \text{if} \quad \widehat{R}_{0K}^{A^*} < 0 \end{cases} . \tag{5}$$

It can be noticed that the value of the laminate's thickness (for both skin and stiffeners laminates), being a multiple of the thickness of the lamina (see the first part of this work), determines directly the number of plies of the laminate. Along with these aspects, we remark that, in the first optimisation phase, we assumed *a-priori* the value of the direction of orthotropy (for every laminate which composes the whole wing box) imposing $\widehat{\Phi}_1^{A^*} = 0$, which means that the orthotropy axis of each laminate has to be aligned with the x axis

of the whole structure. Therefore, for a quasi-homogeneous, fully-orthotropic laminate with given values of polar parameters $\widehat{R}_0^{A^*}$, $\widehat{R}_1^{A^*}$, $\widehat{\Phi}_1^{A^*}$ and $\widehat{K}^{A^*}$, the problem can be stated as (see [1]):

$$\min_{\boldsymbol{\delta}} F(\boldsymbol{\delta}) = \sum_{j=1}^{6} f_j(\boldsymbol{\delta}) \ ,$$

with :

$$\begin{cases} f_1(\boldsymbol{\delta}) = \left(\dfrac{\|\mathbf{B}^*\|}{\|\mathbf{Q}\|} \right)^2 \ , \\ f_2(\boldsymbol{\delta}) = \left(\dfrac{\|\mathbf{C}\|}{\|\mathbf{Q}\|} \right)^2 \ , \\ f_3(\boldsymbol{\delta}) = \left(\dfrac{\Phi_0^{A^*} - \Phi_1^{A^*} - \widehat{K}^{A^*} \dfrac{\pi}{4}}{\dfrac{\pi}{4}} \right)^2 \ , \\ f_4(\boldsymbol{\delta}) = \left(\dfrac{R_0^{A^*} - \widehat{R}_0^{A^*}}{\widehat{R}_0^{A^*}} \right)^2 \ , \\ f_5(\boldsymbol{\delta}) = \left(\dfrac{R_1^{A^*} - \widehat{R}_1^{A^*}}{\widehat{R}_1^{A^*}} \right)^2 \ , \\ f_6(\boldsymbol{\delta}) = \left(\dfrac{\Phi^{A^*}{}_1 - \widehat{\Phi}_1^{A^*}}{\dfrac{\pi}{4}} \right)^2 \ . \end{cases} \tag{6}$$

In eqs. (6), $\boldsymbol{\delta}$ is the vector of layers orientations, while $f_j(\boldsymbol{\delta})$ is the j^{th} partial term of the objective function. The terms $f_1(\boldsymbol{\delta})$ and $f_2(\boldsymbol{\delta})$ are related to the quasi-homogeneity conditions, while the third one, $f_3(\boldsymbol{\delta})$, is linked to the orthotropy condition. The function $f_3(\boldsymbol{\delta})$ takes also into account the prescribed value $\widehat{K}^{A^*}$ of parameter K^{A^*} issued from the first optimisation phase. The terms $f_4(\boldsymbol{\delta})$ and $f_5(\boldsymbol{\delta})$ correspond to the prescribed optimal values $\widehat{R}_0^{A^*}$ and $\widehat{R}_1^{A^*}$ of the polar moduli $R_0^{A^*}$ and $R_1^{A^*}$. Finally, the term $f_6(\boldsymbol{\delta})$ corresponds to the imposed direction of orthotropy of the laminate ($\Phi_1^{A^*} = \widehat{\Phi}_1^{A^*} = 0$, as explained in the structural optimisation phase).

In eqs. (6), $\|\mathbf{B}^*\|$ is the norm of the homogenized coupling tensor, $\|\mathbf{C}\|$ is the norm of the homogeneity tensor, while the normalization factor, $\|\mathbf{Q}\|$, is the one of the layer reduced stiffness tensor. Both norms are calculated using the tensor norm proposed by Kandil and Verchery [21]. All the other polar parameters are referred to $\mathbf{A}^*$ tensor. The normalisation factor of the orthotropy requirement is assumed equal to $\dfrac{\pi}{4}$.

Despite the quadratic form of eqs. (6) is a non-dimensional, positive semi-definite function of the polar parameters of the laminate, it depends upon all the mechanical and geometrical properties of the laminate, i.e. stacking sequences, material and thickness of the plies. In addition, the objective function of eqs. (6) is non-convex in the space of layer orientations, since the polar parameters of the laminate depend upon circular functions of the orientations, as reported in eqs. (2).

Due to the nature of the optimisation problem (6), which is highly non-linear and non-convex, and also due to the nature of the design variables, i.e. plies orientations, that can be continuous as well as discrete, we have chosen a genetic algorithm as numerical strategy to perform the solution search. In this second step of the optimisation process, the new version of the GA BIANCA (see [5, 18]) was also employed. The structure of the genotype of the individual-laminate is shown in Fig. 1. The genotype is made of n chromosomes which

correspond to the number of layers, and each chromosome is composed, on its turn, by a single gene which represents the ply orientation.

4 Numerical results

Since the laminate's elastic behaviour depends upon the elastic properties of the elementary ply, the results must refer to a given material; in this paper, a highly anisotropic unidirectional carbon/epoxy ply (T300/5208) [22] was chosen. Its properties are shown in Table 1.

Three cases were considered, according to the results of the first step of the optimisation process: the first case concerns the wing-box section with identical stiffeners, the second one is about the wing-box section with non-identical stiffeners, while the last one concerns the wing-box section with non-identical stiffeners with a symmetric distribution of geometrical and polar parameters with respect to the global $x - z$ plane of the structure, see Fig. 4. In the first case, since the stiffeners are identical, we have performed only two solution searches for the problem (6): one for the laminate of the skin and another one for the laminate of the stiffeners. Instead, for the last two cases we have performed one simulation for the skin and one simulation for every laminate of each stiffener.

Different types of numerical methods can be used to solve the optimisation problem of eqs. (6). As said previously, to perform the solution search we used the improved GA BIANCA. As reported in eqs. (6) the design variables of our optimisation problem are the layers orientations, which can vary between $-90°$ and $90°$ with a step of $1°$. For every simulation, the population size is set to $N_{ind} = 500$ and the maximum number of generations is assumed equal to $N_{gen} = 500$. The crossover and mutation probability are $p_{cross} = 0.85$ and $p_{mut} = 1/N_{ind}$, respectively. Selection is performed by roulette-wheel operator and the elitism is active.

As in each numerical technique, the quality of solutions found by BIANCA can be estimated on the basis of a numerical tolerance, that is the residual. For a discussion on the importance of the numerical residual in such kind of problems, see [6]. It is worth noting that, being $F(\boldsymbol{\delta})$ a non-dimensional function, the residual of the solution is a non-dimensional quantity, too.

4.1 Wing-box panel with identical stiffeners

Table 2 shows the outcomes of the first optimisation step for the wing-box section with identical stiffeners. Considering that the value of the ply's thickness is 0.125 mm, we can notice that the laminate of each stiffener is made of 29 plies and has the orthotropy with $\widehat{K}^{A^*} = 1$, indeed the value of the polar quantity $(R_{0K}^{A^*})^S$ is negative. Instead, the skin laminate is made of 32 layers and shows the orthotropy with $\widehat{K}^{A^*} = 0$.

Table 3 shows the best stacking sequences found using BIANCA for problem (6). The residual in the last column is the value of the global objective function $F(\boldsymbol{\delta})$ for the solution indicated aside (we remind that exact solutions correspond to the zeroes of the objective function). Fig. 2 shows the first component of the homogenised stiffness tensors of the laminate, i.e. $\mathbf{A}^*$, $\mathbf{B}^*$ and $\mathbf{D}^*$, for stiffeners and skin : the solid line refers to the in-plane behaviour, the dashed one to the out-of-plane stiffness tensor, while the dash-dotted one is linked to the coupling stiffness tensor. We can see that both laminates are uncoupled (the dash-dotted curve shows that B_{11}^* assumes extremely small values, practically null), homogeneous (the solid and dashed curves are practically coincident) and fully-orthotropic (they show two axes of symmetry in the plane). Moreover,

the main orthotropy axis is aligned with the x axis of the structure, in fact it is oriented at 0°. Similar considerations can be done for the other components of these tensors, not shown in Fig. 2.

Fig. 3 shows the trend of the best solution along the generations, for stiffeners and skin laminates, respectively. In particular, we can notice that the best solution is found after 340 generations for stiffeners laminate, while for the laminate of the skin is found after 250 generations.

4.2 Wing-box panel with non-identical stiffeners

Table 4 shows the outcomes of the first optimisation step for the wing-box section with non-identical stiffeners. The number of plies for each laminate, indicated in column 3, is computed considering that the value of the thickness of the elementary layer is 0.125 mm.

Table 5 shows the best stacking sequences found using BIANCA for problem (6). The residual in the last column is the value of the global objective function $F(\boldsymbol{\delta})$ for the solution indicated aside (we remind that exact solutions correspond to zeroes of the objective function). We recall that, since the stiffeners are non-identical, we have solved the problem (6) for each laminate of the stiffeners and the skin. For the sake of brevity we do not show the polar diagrams and the trend of the best solution for stiffeners and skin laminates. Nevertheless, the considerations made for the wing-box section with identical stiffeners can be done for this second case too.

4.3 Wing-box panel with non-identical stiffeners, symmetric distribution

Table 6 shows the outcomes of the first optimisation step for the wing-box section with non-identical stiffeners with symmetric distribution of geometrical and material properties with respect to the global $x-z$ plane of the structure, see Fig. 4. The number of plies for each laminate, indicated in column 3, is computed considering that the value of the thickness of the elementary layer is 0.125 mm.

Table 7 shows the best stacking sequences found using BIANCA for problem (6). The residual in the last column is the value of the global objective function $F(\boldsymbol{\delta})$ for the solution indicated aside (we remind that exact solutions correspond to zeroes of the objective function). We recall that, since the stiffeners are non-identical, we have solved the problem (6) for each laminate of the stiffeners and the skin. For the sake of brevity we do not show the polar diagrams and the trend of the best solution for stiffeners and skin laminates. Nevertheless, the considerations made for the wing-box section with identical stiffeners can be done for this last case too.

5 Verification of the optimal stacking sequences

In this second step of the optimisation process, the finite element analysis is used in order to verify the best stacking sequences found for each stiffener and for the skin laminates, for each of the three cases cited beforehand. The FE model is realised in ANSYS® environment.

Fig. 4 shows the geometry, mesh, loads and boundary conditions of the wing-box FE model. The structure is modelled using SHELL99 elements, with 8 nodes and 6 degrees of freedom (DOFs) per node. This kind of element is well suited for linear and non-linear buckling analyses. Moreover, these shell elements present 3 integration point along the thickness for each ply. It is possible to use them defining the laminate in the explicit or implicit way: through the explicit definition it is possible to define the laminate directly with the

stacking sequence, i.e. plies materials, orientations and thickness, whilst via the implicit definition we define the laminate by means of the classical **A**, **D** and **B** stiffness tensors. Unlike the FE analysis made in the first phase, in this second phase each laminate is defined using the explicit formulation of SHELL99 elements, entering directly the number of plies, the thickness and the orientation of each layer of the laminates of the stiffeners and the skin (as shown in Tables 3, 5 and 7, respectively), besides the linear elastic behaviour for the elementary ply, whose properties are listed in Table 1.

For the rest, the FE model is exactly the same as in the first optimisation phase, namely for what concerns boundary and loading conditions, represented again in Fig. 4. For both the cases of the wing-box section with identical and non-identical stiffeners, the quality of the solution of problem (6) is evaluated comparing the mechanical response (in terms of buckling load and corresponding deformed shape) of this FE model, in which we have entered directly the stacking sequences of the laminates composing the structure, with the mechanical response of the FE model used in the first optimisation phase. Also for this FE model, after a preliminary mesh sensitivity study the average dimensions of the shell elements are chosen equal to 14×14 mm^2. An eigenvalue linear buckling analysis is performed in order to evaluate the first buckling load of the structure.

Concerning the case of the wing-box section with identical stiffeners, Fig. 5 shows the deformed shape of the whole structure for both FE models used in the first optimisation step and in this verification phase. We can see that the deformed shape is identical for both models, while the value of the buckling load of the wing-box section where we set directly the stacking sequences is $p_{cr\,ver} = 1949$ N/mm, which is slightly greater than $p_{cr} = 1943$ N/mm found at the end of the first optimisation step.

Concerning the case of the wing-box section with non-identical stiffeners, Fig. 6 shows the deformed shape of the whole structure for both FE models used in the first optimisation step and in this verification phase. Also in this case, we can see that the deformed shape is practically identical for both models, while the value of the buckling load of the wing-box FE model of the verification phase is increased, i.e. $p_{cr\,ver} = 2124$ N/mm which is greater than $p_{cr} = 1931$ N/mm found at the end of the first optimisation step.

Concerning the last studied case, Fig. 7 shows the deformed shape of the whole structure for both FE models used in the first optimisation step and in this verification phase. Also in this case, we can see that the deformed shape is practically identical for both models, while the value of the buckling load of the wing-box FE model of the verification phase is increased, i.e. $p_{cr\,ver} = 2115$ N/mm which is greater than $p_{cr} = 1933$ N/mm found at the end of the first optimisation step.

5.1 Some remarks on the type of laminate's stacking sequence

In this section we want to highlight the importance of the use of non-standard stacking sequences for composite laminated panels. To do this, we compare the results obtained for problem (6) found in the case of the wing-box section with identical stiffeners, with the ones that can be found using standard stacking sequences often employed in the aeronautical field, i.e. symmetric sequences which can assume only the values $0°$, $\pm 45°$ and $90°$ for plies orientation. In particular, we try to find a solution for the problem (6) of the wing-box section with identical stiffeners, assuming *a-priori* a symmetric stacking sequence and using a set of discrete layers' orientations, which can vary between $-45°$ and $90°$ with a step of $45°$. Even in this case, the aim is to obtain the outcomes of the first optimisation step for the wing-box section with identical stiffeners, shown in Table

2. It can be noticed that, for symmetric stacking sequences the coupling stiffness tensor of the laminate is null, so the first term of eqs.(6) is identically zero.

Concerning the genetic parameters, they are strictly those already used in the previous calculations (see Sec. 4).

Firstly, we conducted two simulations in order to find a solution for the optimisation problem (6) with a given number of layers for the laminates of skin and stiffeners, i.e. 30 and 32, respectively. In this case, the best solution found for the laminate of stiffeners shows a good value for the numerical residual, $F(\boldsymbol{\delta}) = 6.624 \times 10^{-4}$ and then satisfies in a good way the requirements expressed in eqs. (6), whilst the best solution found for the laminate of skin with 32 plies does not reach in a satisfactory way all the elastic requirements, indeed the value of the residual is $F(\boldsymbol{\delta}) = 6.820 \times 10^{-3}$ with the following stacking sequence: $[90/0/90/0_3/90/0/-45/45/90_2/45/90/0_2]_s$.

In order to improve the quality of the solution for the laminate of the skin, we perform several calculations by increasing the number of plies. In particular, we reach the elastic requirements of the optimisation problem (6) with 40 layers within a good precision. Table 8 shows the best stacking sequences found using BIANCA for problem (6) using standard stacking sequences. We can notice that, in order to satisfy all the requirements using symmetric stacking sequences, we need a higher number of layers than the solution shown in Table 3. In particular, we need 30 and 40 plies for the laminates of stiffeners and skin respectively. This means that the solution found using symmetric stacking sequences is not a minimum-weight solution. Indeed, in this case, the weight of the whole wing-box section is 710.23 N, which means an increase of about 20% of the weight of the structure when compared to the non-standard stacking sequence solution shown in Table 3, whose weight is 587.28 N.

Fig. 8 shows the first component of the homogenised stiffness tensors of the laminate, i.e. $\mathbf{A}^*$, $\mathbf{B}^*$ and $\mathbf{D}^*$, for stiffeners and skin: the solid line refers to the in-plane behaviour, the dashed one to the out-of-plane stiffness tensor, while the dash-dotted one is linked to the coupling stiffness tensor. We can see that both laminates are uncoupled (the dash-dotted curve disappears, i.e. B^*_{11} is identically zero), homogeneous (the solid and dashed curves are practically coincident) and fully-orthotropic (they show two axes of symmetry in the plane). Moreover, the main orthotropy axis is aligned with the x axis of the structure, in fact it is oriented at $0°$. Similar considerations can be done for the other components of those tensors, not shown in Fig. 8.

Fig. 9 shows the trend of the best solution along the generations, for stiffeners and skin laminates, respectively. In particular, we can notice that the best solution is found after 40 generations for stiffeners laminate, while for the laminate of the skin it is found after 150 generations.

To remark that the solutions so found are not balanced, as often used to obtain in-plane orthotropy (but not bending orthotropy, as often erroneously thought or implicitly admitted, like in [23]). Nevertheless, they are orthotropic, and not only in extension, but also in bending. The assumption of balanced stacks will obviously lead to a further increase of the final weight of the structure. So, the use of unconventional stacking sequences, as done in this paper, is really more convenient for the reduction of the weight, as stated in the results shown above.

6 Conclusions

A two-step procedure for the design of wing-box composite stiffened panels was presented. The procedure is divided into two phases: the global structural optimisation and the laminate design. In this paper we have shown the results concerning the second optimisation phase, i.e. the optimal design of the laminate.

The problem of designing laminates, having given elastic symmetries and satisfying, simultaneously, the requirements on the polar parameters issued from the structural optimisation phase, is stated as an unconstrained minimisation problem of a positive semi-definite function, whose absolute minimum is known a-priori and it is equal to 0.

Due to the presence of discrete variables, as the orientation of the layers, the use of genetic algorithms appears to be particularly profitable. In particular, the use of the GA BIANCA results very convenient when dealing with such kinds of optimisation problems.

The problem is formulated in the most general case: no simplifying hypotheses are formulated on the types of stacking sequences used for skin and stiffeners laminates: no standard sequences, such as symmetric balanced, angle-ply or cross-ply sequences are employed. In this manner, we have no restriction on the ply's orientation and we perform a real global search of solutions: renouncing the use of standard stacking sequences leads to find some wing-box configurations which show a reduction of the weight of the whole structure up to 50%, when compared with a classical solution realised by aluminium alloy. Moreover, these configurations show good mechanical performances, in terms of pre-buckling stiffness and buckling loads.

In addition, we compared the optimal non-standard stacking sequences found using BIANCA with the standard stacking sequences often employed in the aeronautical field, i.e. symmetric sequences which can assume only the values $0°$, $\pm 45°$ and $90°$ for the orientation of the plies. We have highlighted that the use of non-standard stacking sequences implies, at least, a reduction of 20% of the weight of the structure when compared with the standard aeronautical stacking sequences.

The proposed approach appears to be very flexible and applicable to various engineering problems in which the results are given by complex and expensive models and a high number of analyses is necessary to reach a suitable optimum. Moreover, the procedure has a high level of versatility: more constraints could be easily added to the optimisation problem, e.g. constraints on the strength, yielding or de-lamination of the laminates which compose the structure, without reducing the power and the robustness of the proposed approach.

Acknowledgements

First author is supported by FNR through Aides à la Formation Recherche Grant PHD-09-139.

References

[1] C. Julien. *Conception optimale de l'anisotropie dans les structures stratifiées à rigidité variable par la mèthode polaire-génétiques.* PhD thesis, Institut d'Alembert UMR7190 CNRS -Université Pierre et Marie Curie Paris 6 , France, 2010.

[2] A. Jibawy, C. Julien, B. Desmorat, A. Vincenti, and F. Léné. Hierarchical structural optimization of laminated plates using polar representation. *International Journal of Solids and Structures*, 48:2576–2584, 2011.

[3] A. Vincenti and B. Desmorat. Optimal orthotropy for minimum elastic energy by the polar method. *Journal of Elasticity*, 102(1):55–78, 2010.

[4] P. Vannucci. A new general approach for optimising the performances of smart laminates. *Mechanics of Advanced Materials and Structures*, in press, 2011.

[5] A. Vincenti, M.R. Ahmadian, and P. Vannucci. Bianca: a genetic algorithm to solve hard combinatorial optimisation problems in engineering. *Journal of Global Optimisation*, 48:399–421, 2010.

[6] P. Vannucci. Designing the elastic properties of laminates as an optimisation problem: a unified approach based on polar tensor invariants. *Structural and Multidisciplinary Optimisation*, 31(5):378–387, 2006.

[7] S. Abrate. Optimal design of laminated plates and shells. *Composite Structures*, 29:269–286, 1994.

[8] H. Ghiasi, D. Pasini, and L. Lessard. Optimum stacking sequence design of composite materials part i: Constant stiffness design. *Composite Structures*, 90:1–11, 2009.

[9] H. Ghiasi, D. Fayazbakhsh, D. Pasini, and L. Lessard. Optimum stacking sequence design of composite materials part ii: Variable stiffness design. *Composite Structures*, 93:1–13, 2010.

[10] F. Werren and C.B. Norris. Mechanical properties of a laminate designed to be isotropic. *US Forest Products Laboratory, USA*, report 1841.

[11] H. Fukunaga. On isotropic laminate configurations. *Journal of Composite Materials*, 29:519–535, 1990.

[12] R. Paradies. Designing quasi-isotropic laminates with respect to bending. *Composite Science and Technologies*, 56:461–472, 1996.

[13] P. Vannucci and G. Verchery. A new method for generating fully isotropic laminates. *Composite Structures*, 58:75–82, 2002.

[14] C. Caprino and I. Crivelli-Visconti. A note on specially orthotropic laminates. *Journal of Composite Materials*, 16:395–399, 1982.

[15] M. Grédiac. On the design of some particular orthotropic plates with non-standard ply orientations. *Journal of Composite Materials*, 34:1665–1699, 2000.

[16] P. Vannucci and G. Verchery. A special class of uncoupled and quasi-homogeneous laminates. *Composite Science and Technologies*, 61:1465–1473, 2001.

[17] P. Vannucci and G. Verchery. Stiffness design of laminates using the polar method. *International Journal of Solids and Structures*, 38:9281–9294, 2001.

[18] M. Montemurro, P. Vannucci, and A. Vincenti. A genetic algorithm with crossover on species for structural optimisation. *Computers and Structures*, 2011(Submitted).

[19] G. Verchery. Les invariants des tenseurs d'ordre 4 du type de l'élasticité. *Proc. of colloque Euromech 115, VIllard-de-Lans, (France)*, 1979.

[20] P. Vannucci. Plane anisotropy by the polar method. *Meccanica*, 40:437–454, 2005.

[21] N. Kandil and G. Verchery. New methods of design for stacking sequences of laminates. *Proc. of the computer aided design in composite materials 88, Southampton (UK)*, pages 243–257, 2005.

[22] S.W. Tsai and T. Hahn. *Introduction to composite materials*. Technomic, 1980.

[23] T.A. Sebaey, C.S. Lopes, N. Blanco, and J. Costa. Ant colony optimization for dispersed laminated composite panels under biaxial loading. *Composite Structures*, 94:31–36, 2011.

Tables

Young's modulus E_1 [MPa]	181000
Young's modulus E_2 [MPa]	10300
Shear modulus G_{12} [MPa]	7170
Poisson's ratio ν_{12}	0.28
Density ρ [kg/mm^3]	1.58×10^{-6}
Ply thickness t_{ply} [mm]	0.125

Table 1: Material properties for unidirectional graphite/epoxy ply T300/5208

Design variable	Value
N	22
t^S [mm]	3.625
h^S [mm]	40.0
$(R_{0K}^{A^*})^S$ [MPa]	-984.36
$(R_1^{A^*})^S$ [MPa]	6425.22
t [mm]	4.0
$R_{0K}^{A^*}$ [MPa]	16399.8
$R_1^{A^*}$ [MPa]	1293.26

Table 2: Best values of design variables found using BIANCA for the wing-box FE model in the first optimisation phase, case with identical stiffeners.

Stiffeners		
N. of layers	Stacking sequence	Residual
29	$[-8/28/26/-45/-58/-3/55/-31/76/34/-39/-87/-7/6/30/$ $-12/-21/-51/18/-55/49/-8/18/12/57/44/-27/-79/-18]$	2.996×10^{-4}
Skin		
N. of layers	Stacking sequence	Residual
32	$[-81/7/-3/-12/82/86/-87/20/-6/76/-7/85/-6/90/-7/87/$ $10/-82/-4/-7/-82/18/-11/-84/-83/7/70/85/1/-12/1/89]$	8.445×10^{-5}

Table 3: Best stacking sequences found using BIANCA for the wing-box section in the second optimisation phase, case with identical stiffeners.

Stiffeners					
ID	t^S [mm]	n	h^S [mm]	$(R_{0K}^{A^*})^S$ [MPa]	$(R_1^{A^*})^S$ [MPa]
01	2.75	22	86.5	−7336.27	13651.0
02	4.75	38	55.5	−9565.0	1970.67
03	2.625	21	55.0	−1392.96	15991.2
04	2.125	17	73.5	18888.6	14574.8
05	3.625	29	46.0	−5404.69	2750.73
06	4.625	37	49.0	5701.86	13261.0
07	2.125	17	58.0	5924.73	11249.3
08	2.0	16	65.0	−8450.64	8847.51
09	4.0	32	48.0	14876.8	4495.6
10	4.0	32	43.0	−1578.69	739.0
11	3.0	24	43.5	1801.56	7574.78
12	3.75	30	41.5	8042.03	4290.32
13	3.0	24	59.0	−1095.8	11495.6
14	4.25	34	52.0	17811.3	1149.56
15	4.375	35	54.0	10865.1	2832.84
16	4.0	32	84.0	12536.7	13178.9
17	2.125	17	48.5	3993.16	10633.4
18	3.125	25	48.5	12276.6	14349.0
19	3.0	24	56.0	12610.9	11536.7
20	2.125	17	56.5	−6333.33	7615.84
21	4.375	35	43.0	15322.6	8950.15
22	3.375	27	56.0	17551.3	5994.13
23	3.625	29	41.0	13242.4	7020.53
Skin					
	t [mm]	n		$R_{0K}^{A^*}$ [MPa]	$R_1^{A^*}$ [MPa]
	4.0	32		12945.3	882.70

Table 4: Best values of design variables found using BIANCA for the wing-box FE model in the first optimisation phase, case with non-identical stiffeners.

Stiffeners			
ID	N. of layers	Stacking sequence	Residual
01	22	[28/ − 29/ − 30/28/25/ − 29/ − 29/28/ − 26/42/ − 26/ 26/24/27/ − 29/ − 26/ − 27/25/30/ − 31/ − 22/29]	1.540×10^{-3}
02	38	[40/ − 36/ − 72/ − 38/59/ − 45/24/42/85/ − 20/12/56/ 43/13/ − 41/ − 35/ − 41/45/ − 61/ − 39/56/39/ − 65/7/ 51/ − 70/ − 50/45/ − 28/ − 20/ − 24/45/ − 32/45/41/ − 74/32/ − 31]	3.287×10^{-4}
03	21	[20/20/ − 17/ − 35/ − 16/38/ − 23/ − 24/ − 10/17/ 29/22/19/ − 23/26/ − 27/24/ − 42/ − 18/ − 18/30]	1.881×10^{-3}
04	17	[0/ − 7/0/86/5/2/2/89/2/0/ − 24/1/0/2/ − 87/6/ − 3]	2.134×10^{-3}
05	29	[37/ − 57/ − 3/40/58/ − 44/ − 11/ − 87/50/ − 22/ − 65/ − 38/ − 41/23/ −33/ − 70/18/29/63/41/42/2/61/ − 14/ − 50/87/ − 19/29/ − 48]	2.972×10^{-4}
06	37	[6/8/1/61/ − 45/5/ − 24/22/ − 50/ 6/ − 7/8/7/51/ − 21/ − 34/12/ − 21/ −11/6/33/ − 6/16/78/5/7/ − 6/ − 51/25/ − 4/6/18/ − 42/54/ − 12/ − 20/9]	2.401×10^{-5}
07	17	[5/38/ − 27/ − 56/ − 9/7/60/16/ − 8/7/ − 29/27/9/ − 40/81/ − 8/6]	1.499×10^{-3}
08	16	[−25/ − 47/28/45/ − 16/23/35/1/ − 42/48/ − 41/ − 36/0/ − 33/45/24]	5.560×10^{-4}
09	32	[6/ − 1/3/6/77/ − 74/ − 85/ − 21/71/ − 17/ − 86/ − 1/90/ − 1/67/ − 85/ 83/1/1/3/3/1/3/ − 66/ − 6/23/8/ − 77/ − 11/ − 12/85/83]	1.475×10^{-4}
10	32	[−37/79/36/ − 77/ − 1/ − 43/46/52/ − 35/ − 13/90/30/ − 31/ − 45/ − 3/36/ 69/ − 76/87/89/ − 28/ − 57/51/21/ − 34/35/14/17/9/ − 73/ − 37/71]	1.292×10^{-3}
11	24	[7/65/15/ − 66/ − 10/ − 9/ − 49/ − 45/ − 22/50/13/5/ 70/ − 22/49/17/19/89/6/ − 33/ − 5/ − 5/ − 45/43]	6.809×10^{-4}
12	30	[2/ − 89/81/ − 15/ − 83/ − 50/ − 19/29/6/34/10/4/ − 10/19/75/ −10/86/3/90/ − 69/ − 39/3/ − 32/87/84/51/0/ − 33/4/21]	5.006×10^{-4}
13	24	[34/ − 45/5/5/ − 30/40/28/3/ − 29/ − 9/ − 25/25/ 9/ − 21/ − 24/ − 56/29/20/55/48/4/ − 39/ − 5/ − 15]	1.056×10^{-3}
14	34	[85/ − 4/ − 75/4/ − 2/84/ − 2/83/88/ − 16/6/2/ − 83/0/87/4/3/ 84/ − 7/84/ − 85/ − 74/86/ − 9/15/ − 86/10/1/ − 6/88/ − 3/ − 89/88/5]	1.993×10^{-4}
15	35	[4/ − 79/82/37/ − 2/ − 10/ − 38/ − 70/76/90/10/ − 9/2/ − 2/18/ − 77/ − 5/ 90/ − 3/78/81/ − 21/ − 87/28/9/ − 66/ − 13/45/8/ − 14/82/ − 71/78/ − 2/ − 2]	1.642×10^{-4}
16	32	[12/11/ − 7/5/ − 85/ − 9/ − 14/ − 66/50/ − 5/ − 5/ − 16/2/87/4/3/ 3/ − 8/ − 6/19/17/ − 15/17/ − 9/17/14/ − 67/ − 9/67/ − 12/4/ − 6]	2.829×10^{-4}
17	17	[−19/20/ − 29/20/ − 71/ − 4/35/62/ − 7/ − 8/3/7/ − 45/ − 35/7/70/12]	9.213×10^{-4}
18	25	[13/0/4/ − 23/ − 31/82/18/22/ − 1/2/ − 3/ − 3/ −30/2/3/14/ − 7/18/3/70/ − 77/ − 2/ − 14/ − 6/12]	4.448×10^{-4}
19	24	[2/ − 79/ − 17/27/ − 5/ − 2/ − 5/ − 4/68/ − 5/24/ − 2/ −83/ − 1/4/ − 69/ − 9/8/ − 18/ − 10/25/81/ − 11/7]	3.765×10^{-5}
20	17	[31/46/ − 14/ − 61/ − 38/ − 22/ − 17/25/ − 50/30/47/6/62/28/ − 29/3/ − 44]	7.442×10^{-4}
21	35	[89/ − 10/9/5/5/ − 6/ − 75/58/ − 4/ − 3/ −3/ − 2/73/ − 74/ − 2/ − 86/ − 2/ − 3/ − 1/ − 3/22/22/ − 5 / − 11/ − 6/ − 86/ − 82/ − 6/71/ − 9/16/4/ − 82/5/ − 10]	2.230×10^{-4}
22	27	[−5/7/ − 83/5/10/ − 15/ − 85/75/90/ − 4/ − 4/83/0/ 3/3/3/2/ − 85/ − 85/ − 85/ − 6/1/3/83/7/ − 8/89]	9.292×10^{-4}
23	29	[89/0/12/ − 25/62/10/ − 6/ − 10/ − 1/ − 74/ − 3/ − 1/ − 82/73/ − 86/ 22/ − 1/26/ − 2/86/10/ − 23/ − 8/ − 10/ − 18/ − 81/13/ − 89/9]	3.364×10^{-4}
Skin			
	N. of layers	Stacking sequence	Residual
	32	[3/ − 79/9/ − 12/85/47/78/ − 5/ − 8/ − 78/81/ − 73/85/ − 37/ − 86/ − 4/ −2/ − 90/6/6/ − 90/5/ − 5/25/86/40/ − 8/ − 5/ − 69/90/ − 10/88]	9.595×10^{-5}

Table 5: Best stacking sequences found using BIANCA for the wing-box section in the second optimisation phase, case with non-identical stiffeners.

Stiffeners					
ID	t^S [mm]	n	h^S [mm]	$(R_{0K}^{A^*})^S$ [MPa]	$(R_1^{A^*})^S$ [MPa]
01	4.0	32	40.0	−10642.20	5850.44
02	2.375	19	45.0	−5999.02	9648.09
03	4.875	39	46.5	−3101.66	4844.57
04	2.0	16	57.0	650.049	14266.9
05	4.25	34	42.0	16102.6	8211.14
06	2.5	20	63.0	−1578.69	11557.2
07	4.125	33	82.5	17477.0	4741.94
08	2.625	21	55.5	−16437.0	7102.64
09	3.25	26	52.5	−2990.22	13363.6
10	4.75	38	53.5	−2581.62	6343.11
11	4.625	37	43.5	15619.7	11228.7
12	4.625	37	43.5	15619.7	11228.7
13	4.75	38	53.5	−2581.62	6343.11
14	3.25	26	52.5	−2990.22	13363.6
15	2.625	21	55.5	−16437.0	7102.64
16	4.125	33	82.5	17477.0	4741.94
17	2.5	20	63.0	−1578.69	11557.2
18	4.25	34	42.0	16102.6	8211.14
19	2.0	16	57.0	650.049	14266.9
20	4.875	39	46.5	−3101.66	4844.57
21	2.375	19	45.0	−5999.02	9648.09
22	4.0	32	40.0	−10642.20	5850.44
Skin					
	t [mm]	n		$R_{0K}^{A^*}$ [MPa]	$R_1^{A^*}$ [MPa]
	4.0	32		9527.86	205.279

Table 6: Best values of design variables found using BIANCA for the wing-box FE model in the first optimisation phase, case with non-identical stiffeners with symmetric distribution.

Stiffeners			
ID	N. of layers	Stacking sequence	Residual
01	32	[31/ − 39/35/ − 54/ − 38/ − 12/ − 30/41/20/ − 56/ − 26/55/55/38/37/31/ −30/ − 38/39/ − 9/ − 44/ − 43/ − 44/ − 50/19/8/23/35/50/ − 45/54/ − 23]	3.079×10^{-4}
02	19	[28/ − 33/ − 40/42/ − 23/0/ − 20/26/33/17/ 34/ − 32/ − 39/72/ − 52/8/6/ − 26/36]	1.443×10^{-3}
03	39	[−3/ − 37/39/50/88/29/48/ − 59/9/ − 60/ − 38/3/ − 15/ 25/ − 29/ − 26/ − 7/33/ − 27/ − 36/ − 71/34/57/ − 55/34/81/ 53/50/12/8/8/ − 61/ − 17/76/ − 26/ − 35/ − 1/ − 55/38]	2.731×10^{-4}
04	16	[30/ − 22/ − 28/ − 27/23/5/ − 10/27/ − 14/27/ − 52/ − 13/14/32/ − 22/7]	2.840×10^{-3}
05	34	[10/ − 12/ − 1/6/ − 82/2/ − 11/77/90/ − 86/ − 88/ − 88/ − 3/1/6/ − 19/10/ 46/5/6/ − 65/3/ − 6/1/2/ − 3/ − 16/90/89/ − 18/ − 10/9/87/13]	1.111×10^{-3}
06	20	[−7/26/17/ − 42/69/ − 38/22/ − 19/10/ − 6/ −33/3/36/ − 40/28/1/46/ − 33/17/ − 29]	8.134×10^{-4}
07	33	[5/1/85/ − 4/ − 4/90/ − 86/ − 18/ − 77/8/82/6/ − 3/85/1/7/0/ 81/1/2/79/ − 3/ − 69/ − 87/0/0/ − 90/ − 21/4/2/ − 88/83/5]	2.354×10^{-4}
08	21	[35/33/ − 38/ − 37/35/ − 36/35/ − 38/ − 38/51/ 10/ − 42/34/35/34/34/ − 38/ − 38/ − 36/ − 36/34]	5.446×10^{-3}
09	26	[−39/34/17/ − 21/34/ − 7/ − 23/ − 14/ − 21/24/1/33/39/ 10/ − 46/ − 35/ − 26/26/ − 27/15/27/34/ − 34/ − 24/ − 10/23]	8.928×10^{-4}
10	38	[13/39/ − 57/1/ − 19/ − 55/77/24/10/ − 43/ − 25/55/48/ −78/ − 15/ − 15/ − 23/35/ − 42/33/8/28/ − 55/ − 12/ − 29/ − 80/ 18/61/ − 16/7/37/21/ − 55/64/ − 31/47/ − 4/ − 35]	4.355×10^{-4}
11	37	[16/ − 16/7/ − 1/ − 7/ − 18/85/9/ − 4/ − 81/3/88/ −88/2/0/9/9/ − 4/ − 24/1/ − 8/ − 2/41/ − 2/ −2/ − 2/9/73/ − 4/ − 72/ − 4/83/ − 4/ − 3/ − 89/ − 5/9]	5.915×10^{-4}
12	37	[16/ − 16/7/ − 1/ − 7/ − 18/85/9/ − 4/ − 81/3/88/ −88/2/0/9/9/ − 4/ − 24/1/ − 8/ − 2/41/ − 2/ −2/ − 2/9/73/ − 4/ − 72/ − 4/83/ − 4/ − 3/ − 89/ − 5/9]	5.915×10^{-4}
13	38	[13/39/ − 57/1/ − 19/ − 55/77/24/10/ − 43/ − 25/55/48/ −78/ − 15/ − 15/ − 23/35/ − 42/33/8/28/ − 55/ − 12/ − 29/ − 80/ 18/61/ − 16/7/37/21/ − 55/64/ − 31/47/ − 4/ − 35]	4.355×10^{-4}
14	26	[−39/34/17/ − 21/34/ − 7/ − 23/ − 14/ − 21/24/1/33/39/ 10/ − 46/ − 35/ − 26/26/ − 27/15/27/34/ − 34/ − 24/ − 10/23]	8.928×10^{-4}
15	21	[35/33/ − 38/ − 37/35/ − 36/35/ − 38/ − 38/51/ 10/ − 42/34/35/34/34/ − 38/ − 38/ − 36/ − 36/34]	5.446×10^{-3}
16	33	[5/1/85/ − 4/ − 4/90/ − 86/ − 18/ − 77/8/82/6/ − 3/85/1/7/0/ 81/1/2/79/ − 3/ − 69/ − 87/0/0/ − 90/ − 21/4/2/ − 88/83/5]	2.354×10^{-4}
17	20	[−7/26/17/ − 42/69/ − 38/22/ − 19/10/ − 6/ −33/3/36/ − 40/28/1/46/ − 33/17/ − 29]	8.134×10^{-4}
18	34	[10/ − 12/ − 1/6/ − 82/2/ − 11/77/90/ − 86/ − 88/ − 88/ − 3/1/6/ − 19/10/ 46/5/6/ − 65/3/ − 6/1/2/ − 3/ − 16/90/89/ − 18/ − 10/9/87/13]	1.111×10^{-3}
19	16	[30/ − 22/ − 28/ − 27/23/5/ − 10/27/ − 14/27/ − 52/ − 13/14/32/ − 22/7]	2.840×10^{-3}
20	39	[−3/ − 37/39/50/88/29/48/ − 59/9/ − 60/ − 38/3/ − 15/ 25/ − 29/ − 26/ − 7/33/ − 27/ − 36/ − 71/34/57/ − 55/34/81/ 53/50/12/8/8/ − 61/ − 17/76/ − 26/ − 35/ − 1/ − 55/38]	2.731×10^{-4}
21	19	[28/ − 33/ − 40/42/ − 23/0/ − 20/26/33/17/ 34/ − 32/ − 39/72/ − 52/8/6/ − 26/36]	1.443×10^{-3}
22	32	[31/ − 39/35/ − 54/ − 38/ − 12/ − 30/41/20/ − 56/ − 26/55/55/38/37/31/ −30/ − 38/39/ − 9/ − 44/ − 43/ − 44/ − 50/19/8/23/35/50/ − 45/54/ − 23]	3.079×10^{-4}
Skin			
	N. of layers	Stacking sequence	Residual
	32	[80/ − 9/85/ − 1/ − 63/19/7/14/ − 34/54/ − 59/85/89/ − 83/87/ − 13/ 78/ − 4/ − 90/4/6/71/ − 11/16/ − 70/36/ − 15/ − 70/ − 26/79/13/ − 90]	3.885×10^{-5}

Table 7: Best stacking sequences found using BIANCA for the wing-box section in the second optimisation phase, case with non-identical stiffeners with symmetric distribution.

Stiffeners		
N. of layers	Stacking sequence	Residual
30	$[-45/45/0_3/90/45/-45/45/0/-45/0/-45/0/45/]_s$	6.624×10^{-4}
Skin		
N. of layers	Stacking sequence	Residual
40	$[0/90/0/90/0/90_2/0/45/-45/90/0/90/0/90_2/0_2/90/0]_s$	9.623×10^{-5}

Table 8: Best stacking sequences found by BIANCA for the wing-box section using symmetric stacking sequences, case with identical stiffeners.

Figures

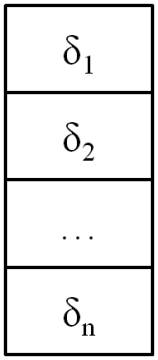

Figure 1: Structure of the individual's genotype for the optimisation problem (6).

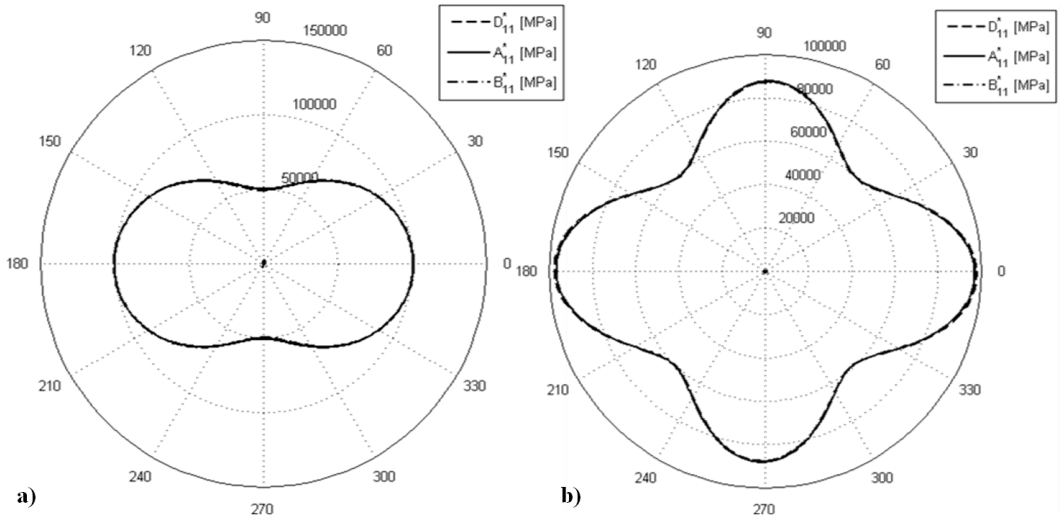

Figure 2: First component of the homogenised stiffness tensors of the laminate for a) stiffeners and b) skin; case with identical stiffeners.

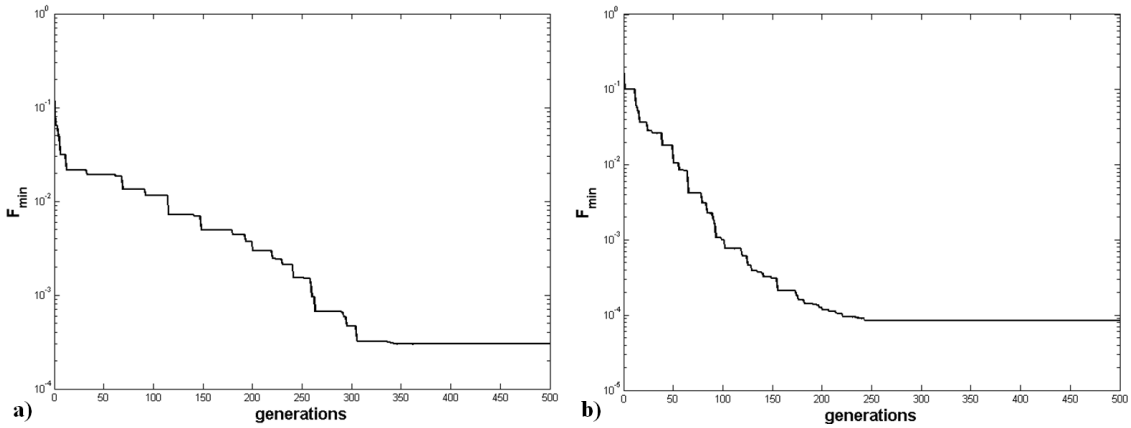

Figure 3: Best values of the objective function along generations for problem (6) for a) stiffeners and b) skin laminates; case with identical stiffeners.

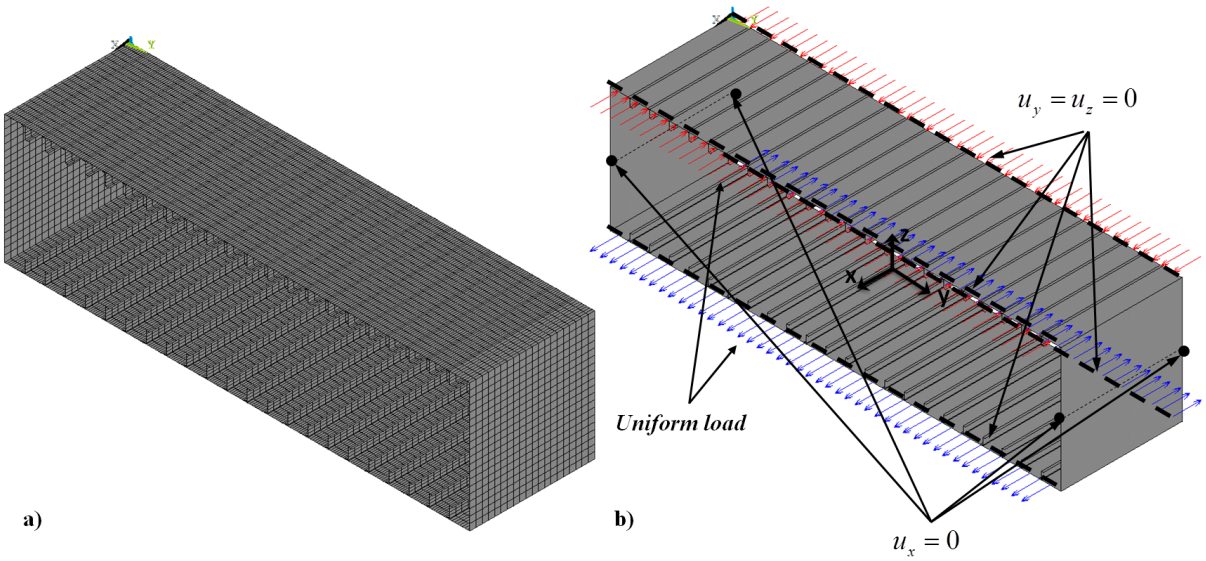

Figure 4: (a) Mesh and (b) loads and boundary conditions for the wing-box FE model.

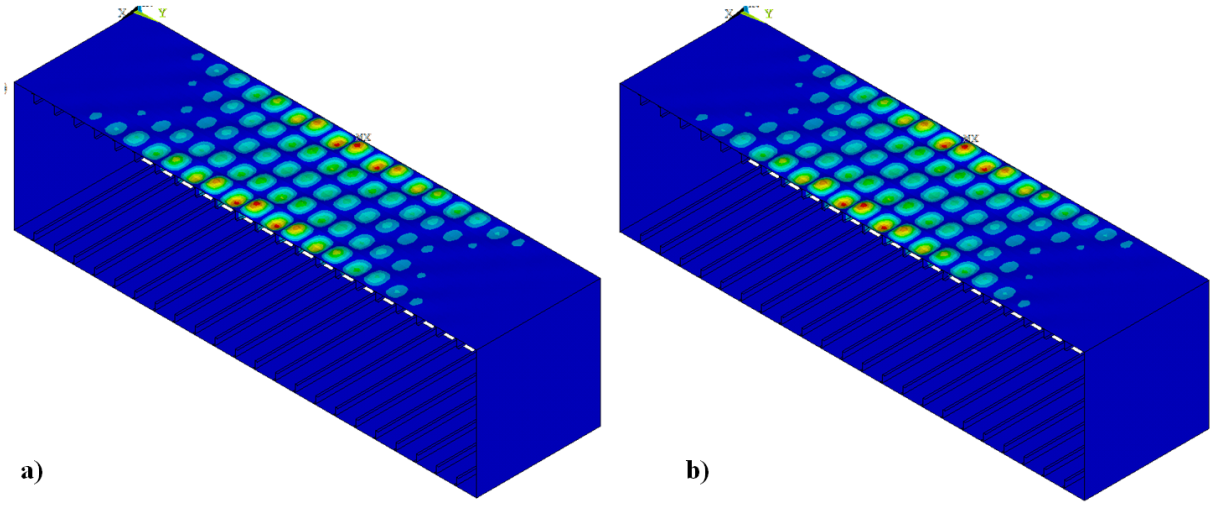

Figure 5: Deformed shape of buckling for the wing-box FE models used in the (a) first optimisation step (homogenised tensors) and in the (b) verification phase (laminates shown in Table 3), case with identical stiffeners.

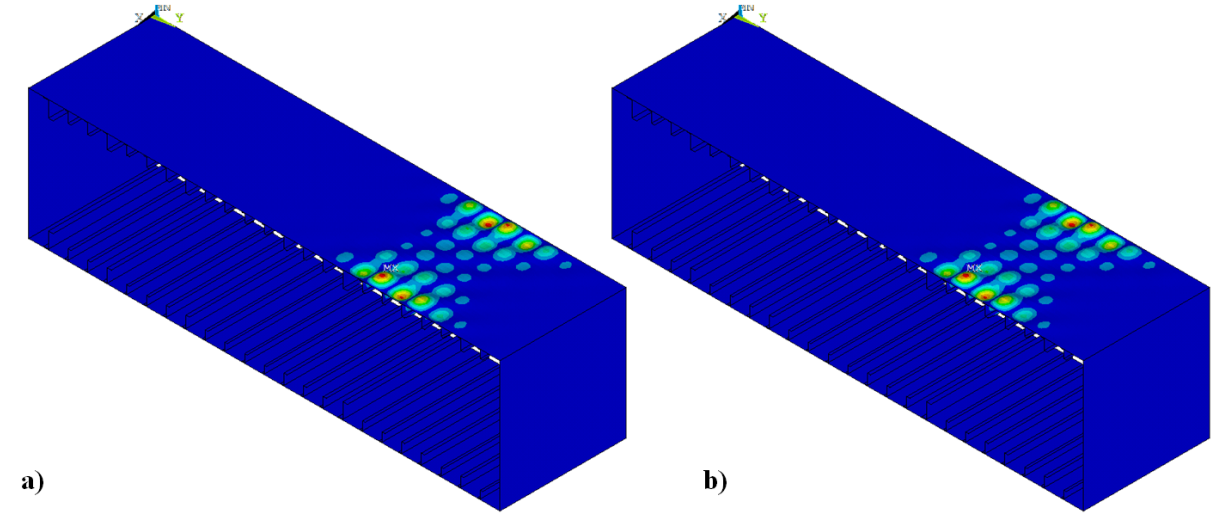

Figure 6: Deformed shape of buckling for the wing-box FE models used in the (a) first optimisation step (homogenised tensors) and in the (b) verification phase (laminates shown in Table 5), case with non-identical stiffeners.

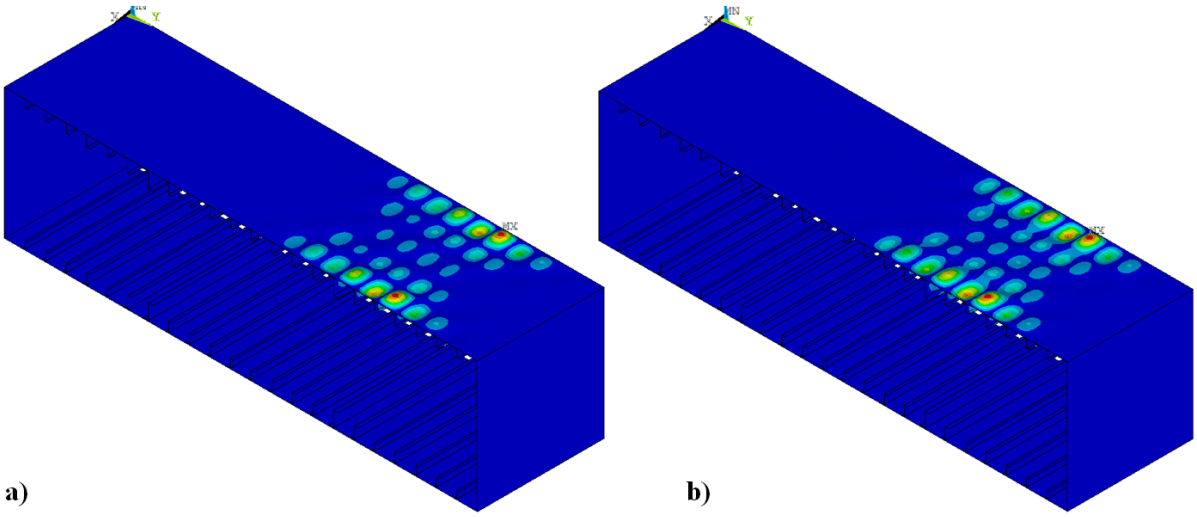

Figure 7: Deformed shape of buckling for the wing-box FE models used in the (a) first optimisation step (homogenised tensors) and in the (b) verification phase (laminates shown in Table 7), case with non-identical stiffeners with symmetric distribution.

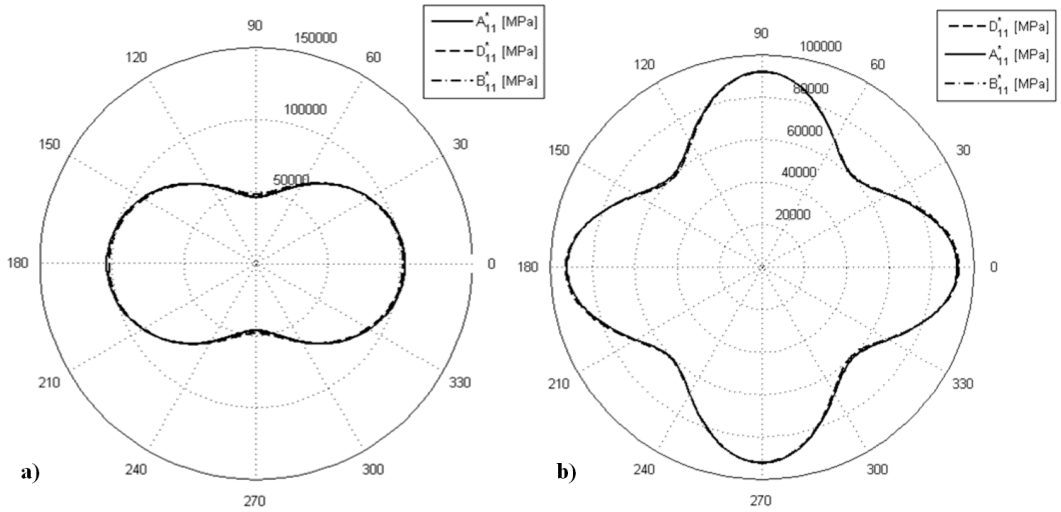

Figure 8: First component of the homogenised stiffness tensors of the laminate with symmetric stacking sequence for a) stiffeners and b) skin; case with identical stiffeners.

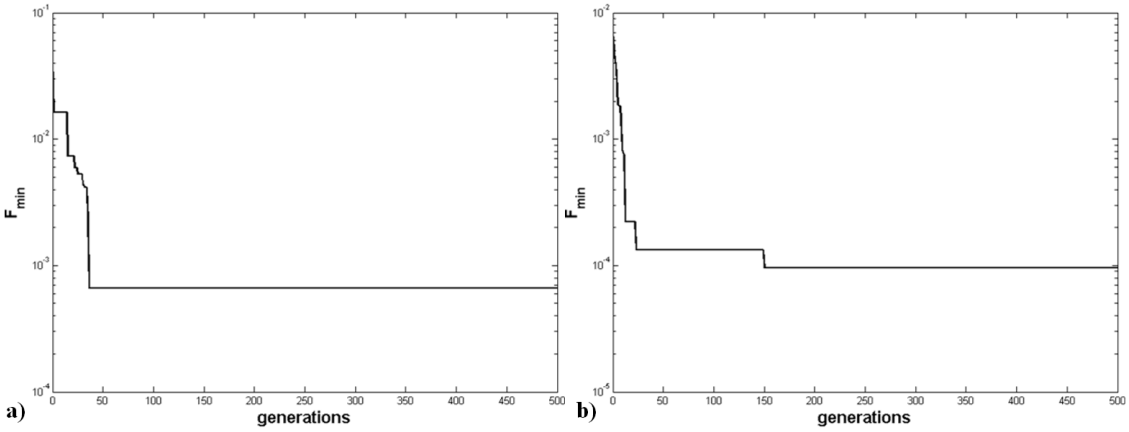

Figure 9: Best values of the objective function along generations for problem (6) using symmetric stacking sequence for a) stiffeners and b) skin laminates; case with identical stiffeners.